EARTH SCIENCES
RESEARCH JOURNAL

Earth Sci. Res. J. Vol. 25, No. 1 (March, 2021): 5-12

UNIVERSIDAD NACIONAL DE COLOMBIA

GEOLOGY

Characterization of hydrothermal events associated with the occurrence of copper-molybdenum minerals in the El Chucho creek at Cerrito, Valle del Cauca-Colombia

Marcela Barrera-Cortes[1] and Juan Carlos Molano Mendoza[1]
[1]Departamento de Geociencias, Universidad Nacional de Colombia, Bogotá-Colombia.
*Corresponding author: dmbarreraco@unal.edu.co; jcmolanom@unal.edu.co

ABSTRACT

At El Chucho creek, located to the west of the Valle del Cauca department in Colombia, some hydrothermal alterations affecting the Buga Batholith rocks and dykes of porphyritic quartz-dioritic and tonalitic composition were identified. These lithological units host mineral occurrences of pyrite, chalcopyrite, and molybdenite that occur disseminated in the rocks or associated with quartz veinlets. The hydrothermal alterations identified were phyllic, propylitic, and, in minor quantity, potassic. The two firsts alterations' distribution is related to structures and pervasive, whereas the last one seems restricted to contact zones of porphyritic dykes on tonalite. Microthermometric data were acquired i) on quartz veinlets of 1 cm thick over a phyllic alteration zone, and ii) on quartz veinlet of 1 cm thick with chalcopyrite ± molybdenite and copper silicates, both veinlets cutting the phaneritic tonalite. Those data suggest that the mineralizing fluids have an aqueous-saline chemical system and were trapped under low volatile content. The microthermal data allowed authors to identify two mineralizing events. One of them of higher temperature, with homogenization temperatures between 275°C-480°C; as the second event is characterized by lower homogenization temperatures that range from 100°C to 139°C.

Keywords: Buga Batholith; hydrothermal alteration; molybdenite; microthermometry; porphyritic dykes.

Caracterización de eventos hidrotermales asociados con ocurrencias de minerales de cobre-molibdeno en la quebrada El Chucho, Cerrito, Valle del Cauca-Colombia

RESUMEN

En la quebrada El Chucho, localizada en el occidente del departamento del Valle del Cauca-Colombia, fueron identificadas alteraciones hidrotermales que afectan tanto a rocas tonalíticas del Batolito de Buga como a diques porfiríticos de composición cuarzo-diorítica y tonalítica. Estas unidades litológicas hospedan minerales como pirita, calcopirita y molibdenita que se presentan diseminados y en parte asociados con vetillas de cuarzo. Las alteraciones hidrotermales identificadas corresponden a fílica, propilítica y en menor medida potásica. La distribución de las dos primeras alteraciones está relacionada con estructuras o bien pueden presentarse de forma pervasiva en las rocas afectadas; mientras que la última parece estar restringida a las zonas de contacto de los diques porfiríticos con la tonalita del Batolito de Buga. Los datos de microtermometría se midieron i) en vetillas de cuarzo de 1 cm de espesor localizadas sobre zonas de alteración fílica y ii) en vetillas de cuarzo de 1 cm de espesor con calcopirita ± molibdenita y silicatos de cobre; ambas vetillas se encuentran cortando la tonalita fanerítica. Los datos microtermométricos sugieren que los fluidos mineralizantes tienen un sistema químico acuoso-salino y fueron atrapados bajo un régimen de bajo contenido volátil; además, la información microtermométrica permitió identificar dos eventos mineralizantes, uno de ellos de alta temperatura, cuyas temperaturas de homogenización varían entre 275°C–480°C y un segundo evento caracterizado por bajas temperaturas de homogenización que van desde 100°C a 139°C.

Palabras clave: Batolito de Buga; alteraciones hidrotermales; molibdenita; microtermometría; diques porfiríticos.

Record
Manuscript received: 17/04/2019
Accepted for publication: 21/09/2020

How to cite item
Barrera-Cortes, M. & Molano, J. C. (2021). Characterization of hydrothermal events associated with the occurrence of copper-molybdenum minerals in the El Chucho creek at Cerrito, Valle del Cauca-Colombia. *Earth Sciences Research Journal*, 25(1), 5-12. DOI: https://doi.org/10.15446/esrj.v25n1.79152

Introduction

The study area is located on the west side of the Central Cordillera of Colombia in the Valle del Cauca department, approximately 14 km to the East of El Cerrito municipality (Figure 1). Nivia (2001) mentioned that the region's geology had been considered suitable for the location of mineral deposits.

The Buga Batholith, a predominant unit on this region, host epigenetic Au-Ag mineralization and, according to Cediel & Shaw (2019), "were accreted to the Colombian margin along with slivers of Farallon – Caribbean Colombian Oceanic Plateau (CCOP) oceanic lithosphere in the Late Cretaceous-Paleocene, during the collision of the leading or lateral edge of the CCOP, along the continental margin."

Nonetheless, most of the metallogenetic studies concerning the Buga Batholith have been focused on Ginebra and Buga's municipalities, located to the northwest of the study area. This work contributes to the knowledge of mineral occurrences identified at the southeastern corner of the area defined by Lopez et al. (2018) as the Ginebra sliver, using cartographic, petrographic, and microthermometric data.

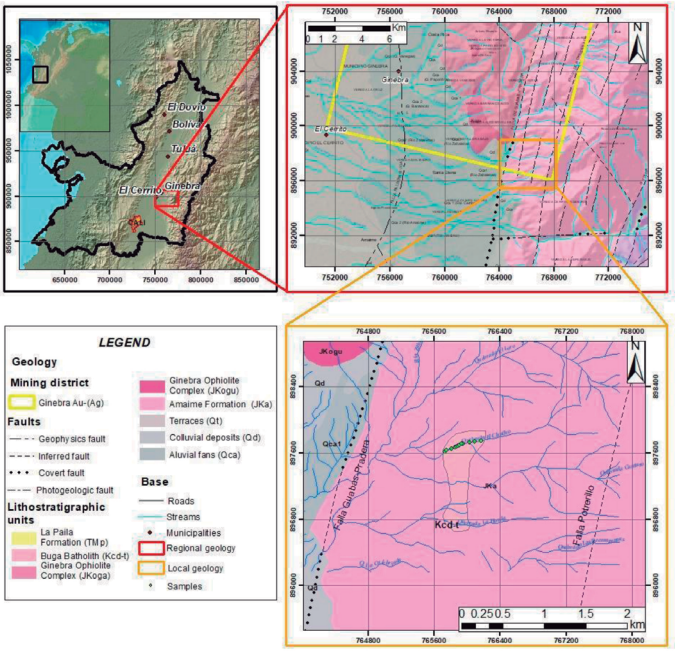

Figure 1. Localization of the study area. Modified from McCourt (1984)

Regional Geology

Litho-tectonically, the study area is located on the Pacific Assemblage Terrane (PAT) of the Western Tectonic Realm (WTR) terrane of Cediel et al. (2003). According to the author, this assemblage of possible allochthonous terranes contains mafic-ultramafic complexes, ophiolite sequences, and oceanic sediments that have been affected by multiple phases of tectonic reworking and translation that among others get to an obduction/accretion of the marginal basin assemblage along the paleocontinent.

The main lithostratigraphic units in this region are the Buga Batholith, the Amaime Formation, and the Ginebra Ophiolite Complex, as McCourt (1984), Nivia (2001) reported.

The Buga Batholith is a polyphase pluton (Leal-Mejía et al., 2018) with a composition that changes between hornblende quartz diorite to tonalite (McCourt, 1984). In the interest area, tonalite is the predominant lithology. Paz et al. (2017) concluded that this batholith mixes partially crystallized granitic magma and a mafic magma upon conducting field relationships and petrographic analysis.

Villagómez et al. (2011) placed these rocks in the transition of calc-alkaline to tholeiitic series. According to Tarazona et al. (2017), the Buga Batholith is a syn-tectonic pluton that approached and reworked pre-exist anisotropic structures to migrate and emplaced into the Ginebra Ophiolite Complex. An U/Pb LA-ICPMS on zircon age of 98.79 ± 0.43 Ma by Brito et al. (2010) and Villagómez et al. (2011) suggest a crystallization age for this pluton of 90.6 ±1.3 Ma and 92.1 ± 0.8 Ma U/Pb (Zircon). Afterward, Nivia *et al.* (2017) dated the Buga Batholith through U/Pb in zircon and got two different ages (88 ± 1.64 Ma and 69 ± 1.41 Ma). Based on these ages, Nivia et al. (2017) has classified the Buga Batholith on two differetn intrusive bodies.

The Amaime Formation was defined by McCourt (1984) as massive tholeiitic basalt with horizons of pillow lavas and local komatiitic basalts, and mention that it is intruded by the plutonic rocks of the Buga Batholith. For Moreno & Pardo (2003), this unit is known as Amaime-Chaucha Complex. They suggested that it is composed of a core of ophiolitic suite intruded by granitoid igneous rocks; besides, pillow and massive basalts of oceanic plateau type are tectonically associated. Nivia (2001) defined the eastern's limit of the unit in the main fault of the Cauca-Almaguer Fault System.

Armas (1984) suggested a pre-Aptian age for these rocks according to the radiometric K/Ar age presented by Brook (1984) for the plutonic rocks of the Buga Batholith (99 ± 4 Ma) that intruded the Amaime Formation. Moreno & Pardo (2003) gave reference to $^{40}Ar/^{39}Ar$ radiometric data from basalts of this unit that provide an age Cenomanian-Turonian.

The Ginebra Ophiolite Complex was defined by Nivia (2001) as an elongated block of ultramafic rocks with an N-S orientation and a 40km length; the eastern contact is faulted (Guabas-Pradera Fault) with the Amaime Formation and is intruded by the Buga Batholith. The western contact is given by the Palmira-Buga Fault that separates it from Miocene sedimentary units. Espinosa (1985), cited by Nivia (2001), described this unit as a sequence of peridotites, banded gabbros, microgabbros, metabasalts, tuffs, microbreccias, and hyaloclastites, cut by dolerite dikes and plagiogranite veinlets.

Besides, Tarazona et al. (2017) identified the following chronologic polyphase history of the complex: i) crystallization, ii) metamorphism on amphibolite facies, iii) milonitization, iv) mylonitic foliation 1, and v) mylonitic foliation 2.

McCourt (1984) mentioned that this complex was intruded by the Buga Batholith and considered that the radiometric ages of this plutonic body of 113 ± 10 Ma (K/Ar on hornblende, Toussaint et al., 1978), 99 ± 4 Ma (Rb/Sr on biotite, Brook, 1984) and 114 ± 3 Ma (discordant minerals aged K/Ar, Brook, 1984) suggest that the intrusion of this pluton on the Ginebra Ophiolite Complex was before 100 Ma and assume the age of the intruded unit as Early Cretaceous or Jurassic.

Later in 2017, Nivia et al. reported ages Ar/Ar of 140.28 ± 3.12 Ma (on clinopyroxene) for gabronorites and 90.84 ± 0.78 Ma (on hornblende) for anphilites. These ages are interpreted as crystallization age and reworked age by the Buga Batholith's intrusion on the Ginebra Ophiolite Complex.

Regional Structures

The geographic location of the study area in the WTR of Cediel et al. (2003), composed by a melange of allochthonous terranes (e.g., PAT), gives to the site an intense tectonic deformation that is represented locally by a set of principal faults (i.e., N20-30E; N60-70E; N40-50W). That accommodates the deformation generated into western Colombia's accretionary complex; these faults have a history of complex and multiple events that mainly correspond with significant scale strike-slip movements (Nivia, 2001).

In the study area, the most relevant fault systems correspond to systems N20-30E and N40-50W; the former is known as the "Palestina" type (Lozano, 1986 cited by Nivia, 2001) that places in contact different lithological units defining principal lithological provinces and is compound of the west to east among others by the Palmira-Buga Fault and Guabas-Pradera (Potrerillo) Fault. The latter system is nominated as "Salento" type by the same author and correspond to an echelon arrangement of sinistral faults that move the trace of the N20-30E faults; McCourt (1984) suggested that some of those faults correspond to tensional brittle structures, an idea that authors have used as Sillitoe (1974) to explain the occurrence of metallic deposits on the Andean Mountains.

Methodology

A detailed geologic mapping (1:800 scale) was carried out over a transect of 500 m along the El Chucho creek using the "Anaconda Mapping Method" described by Einaudi (1997). A total of twelve thin-polished sections were analyzed to get a petrographic classification based on the modal abundance of primary minerals and identification of alteration minerals; two of the sections were made as doubly polished thin sections for fluid inclusions purposes. All units were analyzed using an Olympus BX-41 polarizing microscope with transmitted and reflected lights.

Modal mineralogy was determined by point counting of 100 points per thing section, and in the case of hydrothermal alteration, the alteration minerals were attributed to primary minerals from which they were formed; the recommendations of Whitney & Evans (2010) for abbreviations form mineral names, and the guidance of the Subcommission on the Systematics of Igneous Rocks (Streckeisen, 1976) were followed for petrographic characterization.

Microthermometric measurements in fluid inclusions were carried out in the National University of Colombia laboratories, Bogotá, using a Linkam THSM 600 stage coupled to an Olympus BX41 petrographic microscope. The equipment accuracy was estimated at +1°C to the lowest temperature and +4.7°C for the highest; the heating and cooling rate are 150ºC/min and 100ºC/min respectively, researching temperatures of -196°C to 600°C. Three-phase changes were recorded during the cooling/heating routines: (1) Eutectic temperature (Te), (2) final ice melting temperature (TmIce), (3) homogenization temperature (Th).

The compositions of mineralizing fluids were modeled by the BULK program from Fluids package (Bakker, 2003; Bakker & Brown, 2003), using the equations for salinity calculation, given by Bodnar (1993) and the state equation of Zhang & Frantz (1987) for estimating the type of components in the inclusions.

Results

Geologic Mapping

In the El Chucho creek, the predominant lithology is a moderated magnetic, light pinkish coarse, equigranular, phaneritic rock, composed mainly of subhedral plagioclases (30 % vol), anhedral quartz (25 % vol), and subhedral hornblende (20 % vol). The mineral occurrences (pyrite, chalcopyrite, and traces of molybdenite) are disseminated in thin quartz veinlets (≤ 1cm) (3 veinlets); all of them complete almost 5 % vol; finally, alteration minerals such as carbonate, chlorite, epidote, sericite and locally biotite (near to dykes intrusions) complete 20 % vol; this mineral composition allow for classifying the rock as tonalite. It is frequent to find lobular contacts with greenish-grey aphanitic basalts, with disseminated fine-grained pyrite, chalcopyrite, and magnetite completing all of them (3 % vol); those rocks are spatially correlated with the Buga Batholith.

In the mapped area, this tonalite is intruded by five porphyritic dykes (45/040; 59/071; 70/135; 70/135 and 44/090)[1] of grey to dark brown color, with aphanitic matrix (~70 % vol) and phenocrysts (~30 % vol) of plagioclase and hornblende of < 1cm, besides of disseminated moderate alteration of carbonate + sericite and pyrite and chalcopyrite disseminated and/or in quartz veinlets occasionally with molybdenite (1 veinlet) and rarely gypsum veinlets < 1 cm thick (1 veinlet); those dykes have two to three meter thick and compositionally are quartz-dioritic to tonalitic.

These sub-volcanic pulses could have given path to fluids that generated a moderate hydrothermal alteration that affected mainly the tonalitic host rock. The identified hydrothermal alteration are (1) moderate propylitic alteration, with a pervasive distribution and in a minor quantity present as straight veinlets of Ep + Qz + Cb ± Chl ± Py ± Mag, sulphurs and oxides as Py, Ccp and Mag are disseminated on the rock; (2) moderate phyllic alteration (seems related with local faults), with mineral association Qz + Ser + Py ± Chl and straight veinlents of Ccp and D-type veinlets (Gustafson & Hunt, 1975), this alteration affects an important portion of the phaneritic tonalite; (3) local very weak potassic alteration, characterized by scarce secondary biotite disseminated on the phaneritic tonalite near to contact zones with porphyritic dykes; also it is possible to find ore minerals as Ccp (3 % vol) and Mol (1 % vol) in B-type veinlets (Gustafson & Hunt, 1975) and disseminated.

Structurally, the zone is controlled by a fragile regime where it is possible to recognize four principal oblique faults (1) N75E/75SE, (2) N80W/53SE, (3) N55E/76NW and (4) N80W/58NW; the first and second with normal sinistral movement and the third and fourth normal dextral movements (Figure 2 and Figure 3).

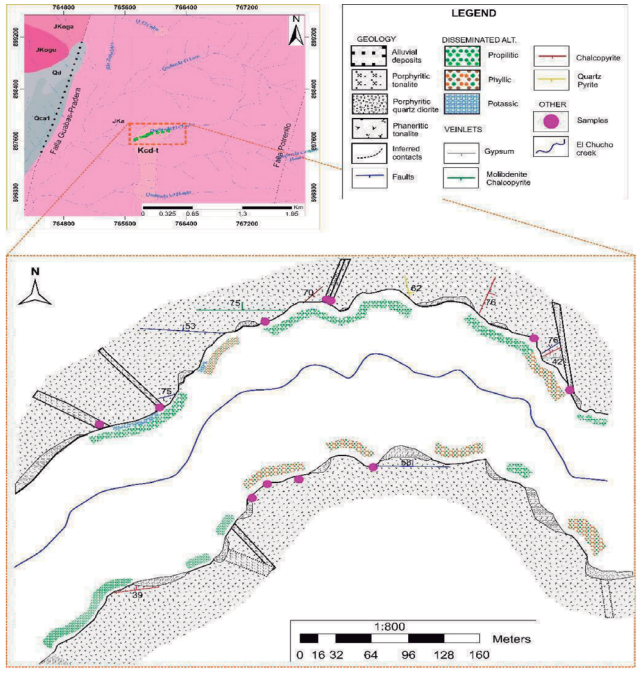

Figure 2. Detailed anaconda map of the El Chucho creek, showing the lithology, hydrothermal alteration, faults and veinlets.

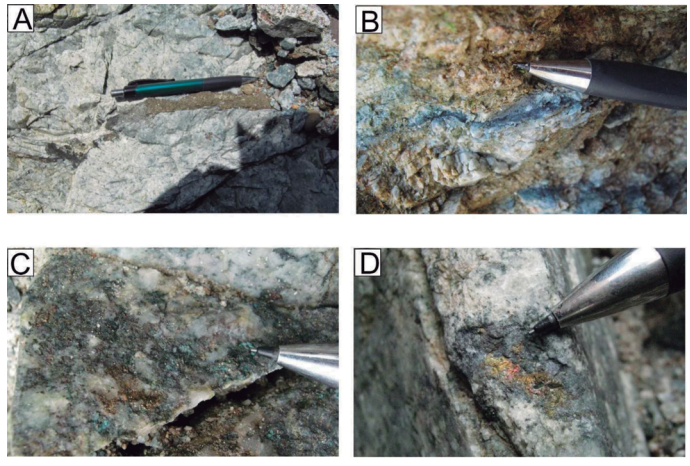

Figure 3. Mineralization styles at the El Chucho creek in phaneritic tonalite. A. Sinuous chalcopyrite veinlet, B. B-type veinlet with suture of chalcopyrite and molybdenite. C. Disseminated molybdenite and chalcopyrite with supergene malaquite. D. Patch of chalcopyrite with supergene bornite and chalcocite.

[1] Structural data for the five porphyritic intrusion, notation on dip/dip direction.

Petrographyc Analysis

Table 1 and Figure 4 present the data used for modal rock classification.

Table 1. Modal mineral percentage of the phaneritic and porphyritic rocks at El Chucho creek

Unita	To Ph						To Po					Qd Po
Mineralb	Mbch07	1247	1257	1260	1261	1262	Mbch04	Mbch05	Mbch09	Mbch11	1258	Mbch08
Qz	29	20	26	38	40	20	27	21	8	10	10	5
Afs	2	0	0	0	3	0	3	0	0	0	0	0
Pl	41	33	44	14	35	0	40	26	27	36	14	28
Chl	10	7	10	11	6	17	7	8	0	10	26	18
Ep	7	0	0	6	0	0	8	6	0	0	0	15
Cb	0	2	2	7	0	20	10	32	30	14	6	14
Py	0	3	2	14	0	3	3	4	0	5	3	2
Ccp	3	1	2	0	5	0	2	3	3	0	0	2
Cct	1	0	1	0	0	0	0	0	1	0	0	0
Mol	0	0	0	0	0	0	0	0	0	0	0	1
Cv	0	0	1	0	0	0	0	0	0	0	0	0
Ser	7	30	0	0	11	40	0	0	0	8	34	15
Bt	0	0	0	0	0	0	0	0	22	8	0	0
Bt 2	0	2	0	0	0	0	0	0	0	0	2	0
Hbl	0	2	4	10	0	0	0	0	9	9	5	0
Cpx	0	0	8	0	0	0	0	0	0	0	0	0
Spn	0	0	0	0	0	0	Trace	0	0	Trace	0	0
Zrn	0	0	0	0	0	0	0	0	0	Trace	0	0
Total	100	100	100	100	100	100	100	100	100	100	100	100
Phenocryst (%)	--	--	--	--	--	--	20	20	20	20	25	20
Matrix (%)	--	--	--	--	--	--	80	80	80	80	75	80

[a] Unit abbreviation: To Ph = Phaneritic tonalite, To Po = Porphyritic tonalite, Qd Po = Porphyritic Quartz-diorite.
[b] Mineral abbreviation: Qz = quartz, Afs = Alkali feldspar, Pl = Plagioclase, Chl = Chlorite, Ep = Epidote, Cb = Carbonate, Py = Pyrite, Ccp = Chalcopyrite, Cct = Chalcocite, Mol = Molybdenite, Cv = Covellite, Ser = Sericite, Bt = Biotite, Bt 2 = Secondary biotite, Hbl = Hornblende, Cpx = Clinopiroxene, Spn = Sphene, Zrn = Zircon.

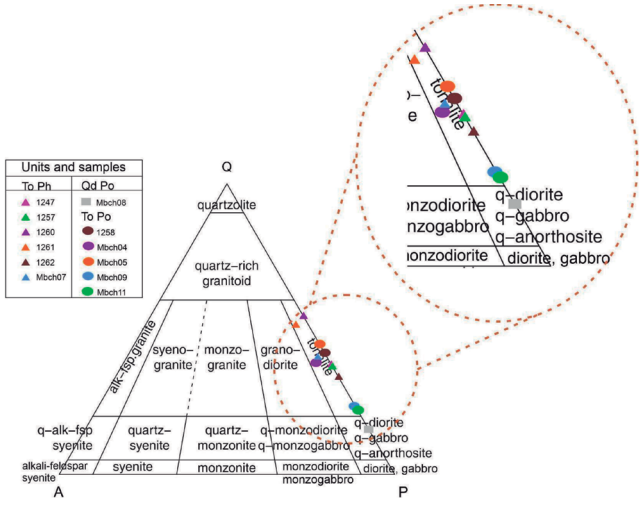

Figure 4. Streckeisen (1976) diagram for modal classification of felsic and intermediate plutonic rocks. Sample classification based on point counting (n = 100). To Ph = Phaneritic tonalite, Qd Po = Porphyritic Quartz-diorite and To Po = Porphyritic tonalite.

Tonalites

These rocks are holocrystalline with anhedral to subhedral crystals and appear with phaneritic (1) and porphyritic (2) texture, that are described as follow:

(1) The phaneritic phase (samples 1247, 1257, 1260, 1261, 1262 and Mbch07), is holocrystalline with subhedral to anhedral crystals, plagioclase is the most abundant mineral (45 to 67 % vol) (An33)2 with antipertitic texture, quartz (33 to 54 % vol) with local mirmequitic texture, alkali feldspar (≤ 4 % vol), hornblende (~3 % vol), less than 1 % vol of pyroxene, pyrite and chalcopyrite (6 % vol) disseminated and in quartz veinlets (≤ 1 cm thickness). Sericite is a common alteration product of plagioclase, while epidote, chlorite and carbonate are frequently alteration product of both, plagioclase and hornblende; scarce secondary biotite appears as a substituent of hornblende (Figure 5 A and B).

(2) The porphyritic phase (samples 1258, Mbch04, Mbch05, Mbch09 and Mbch11) has a fine to medium-grained matrix (75 % vol) composed of crystals of plagioclase, quartz, alkali feldspar and hornblende; phenocrysts (25 % vol) consists of medium to coarse grained subhedral to anhedral crystals of plagioclase (55 to 78 % vol) (An32), quartz (22 to 45 % vol), hornblende (<9 % vol) and alkali feldspar (<4 % vol). Plagioclase as well as hornblende are altered to carbonate, chlorite, epidote and secondary biotite (scarce); sulphide minerals as pyrite and chalcopyrite (~3 % vol) are present disseminated and in quartz veinlets (≤ 1 cm thickness). Sphene and zircon are accessory minerals (Figure 5 C and D).

Quartz diorite

This rock (sample Mbch08) is holocrystalline with a porphyritic medium to fine-grained texture, and has a criptocrystalline matrix (80 % vol) composed by plagioclase, quartz, magnetite and chalcopyrite; the phenocrysts (20 % vol) are mainly of euhedral plagioclase (An10) (28 vol %) with sericitic alteration, subhedral quartz (5 vol%) and (20 vol%) of euhedral to subhedral hornblende altered to chlorite, epidote and carbonate. Sulphide minerals as pyrite,

[2] Composition calculated by Michel Lévy method

chalcopyrite and molybdenite (4 % vol) are disseminated into B-type veinlets (Figure 5 E and F).

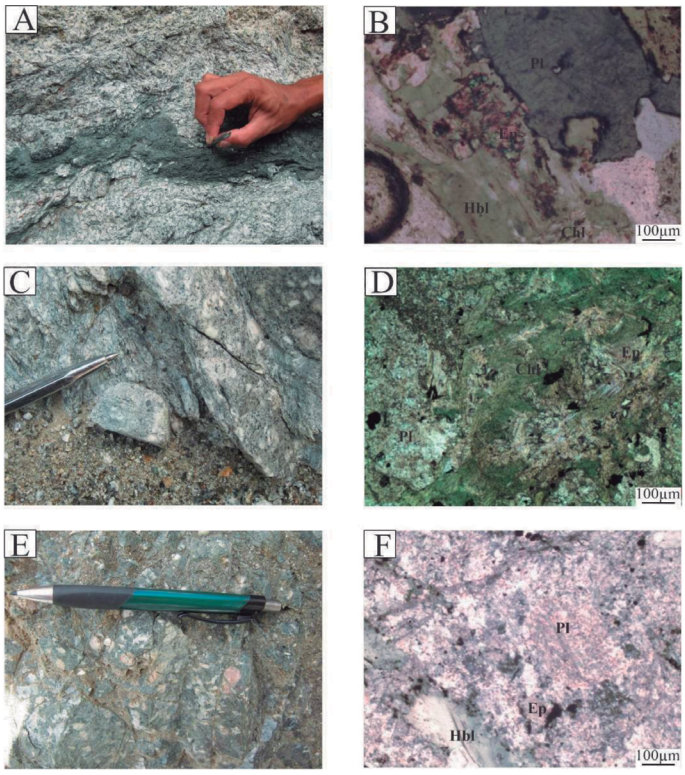

Figure 5. Macroscopic and microscopic aspect of different lithologies at the El Chucho creek. A and B. Phaneritic tonalite. note in A the medium grained phaneritic texture and the ductil deformation showed mainly in the basaltic flux. On B it is possible to observe the alteration to Ep and Chl on the Hbl crystals. C and D. Porphyritic tonalite with phenocrysts of plagioclase and hornblende. This rock has been moderately altered to propylitic assemblage. E and F. Porphyritic quartz-diorite with phenocryst mostly of plagioclase affected by strong Phyllic alteration. Mineral abbreviation: Pl=Plagioclase, Hbl=Hornblende, Ep=Epidote, Chl=Chlorite.

Microthermometry Analysis

Fluid inclusions characteristics

The occurrence of two types of fluid inclusions assemblages was stablished, Table 2 shows the characteristics and the average microthermometric and salinity data for both types of fluid inclusions.

Type I fluid inclusions are common in sample 1262 (phaneritic tonalite), those fluid inclusions were measured in a veinlet of 1 cm thick, compound only by quartz, over a zone of phyllic alteration. Type II fluid inclusions are typical

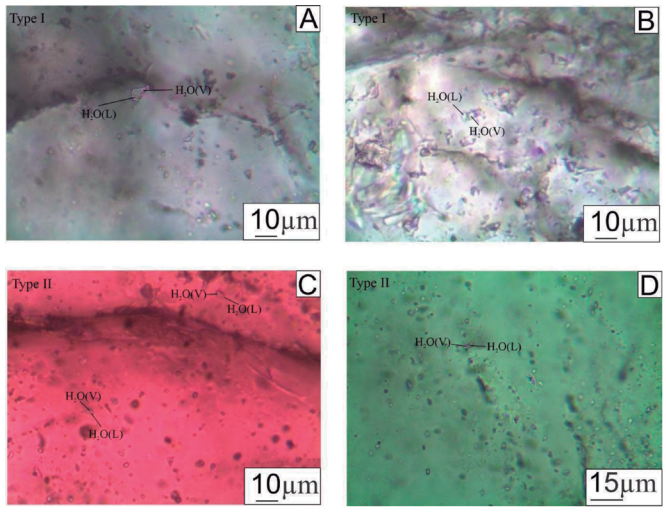

Figure 6. Fluid inclusion types in quartz crystals at El Chucho creek. A. Type I fluid inclusion with ovoid shape and a size of 10 µm, rock sample 1262, B. Biphasic type I fluid inclusion with irregular shape and 8 µm in size, rock sample 1262. C. Small biphasic type II fluid inclusion with ovoid and irregular shapes and <5 µm in size, rock sample 1257. D. Type II fluid inclusion from 4 to 6 µm in tabular, amorphous and ovoid shapes, rock sample 1257.

in sample 1257 (phaneritic tonalite), and are found in 1 cm thick quartz veinlet with chalcopyrite and copper silicates, associated with molybdenite.

Type I inclusions: Primary, biphasic aqueous FI found at the centre or growth zone of crystals, with ovoid and irregular shapes, whose size vary between 4 - 11 µm and L/V ratio between 12 – 89.

Type II inclusions: Primary, biphasic aqueous FI found mainly at the centre zone of crystals, whose shapes vary among ovoid, irregular and tabular, the size of the inclusion vary between 4 - 9 µm and the L/V ratio is between 14 – 44. (Figure 6).

Microthermometric Results

These results are presented separately according to the fluid inclusion type; the composition, and salinity of both type of inclusions were modeled on the BULK program from Fluids package (Bakker, 2003; Bakker & Brown, 2003).

Type I fluid inclusions: The first observed change of phase corresponds to the first melting temperature of ice (Te) ranging from -46 to -15°C with a major data concentration at -35.2°C. Ice final melting temperature (TmIce) ranging from -4.5 to -1.2°C; all inclusions homogenize (Th) to liquid phase (L+V→L) at a temperature ranging from 125 to 480°C with an important data concentration at an approximate temperature of 285°C. These data indicate a salinity of 7.2 to 2.1 wt % NaCl equivalent (eq.) (4.7 on average) (Figure 7).

Table 2. Petrographic and microthermometric data of fluid inclusions at El Chucho creek.

Type	Size (µm)	Shape	Phases	L/V ratio	Composition	Microthermometric data[a]			Salinities[b]
						Eutectic T (°C)	Ice Melt T (°C)	Homog. T (°C)	
I	4–11	Ovoid and Irregular	L/V	12–89	H2O - MgCl2	-30,47	-2,66	291,14	4,7
II	4–9	Ovoid, Irregular, Tabular	L/V	14–44	H2O - NaCl - KCl	-26,89	-2,45	121,7	4,8

a and b data correspond to the average of the data measured and calculated on each type of fluid inclusion.

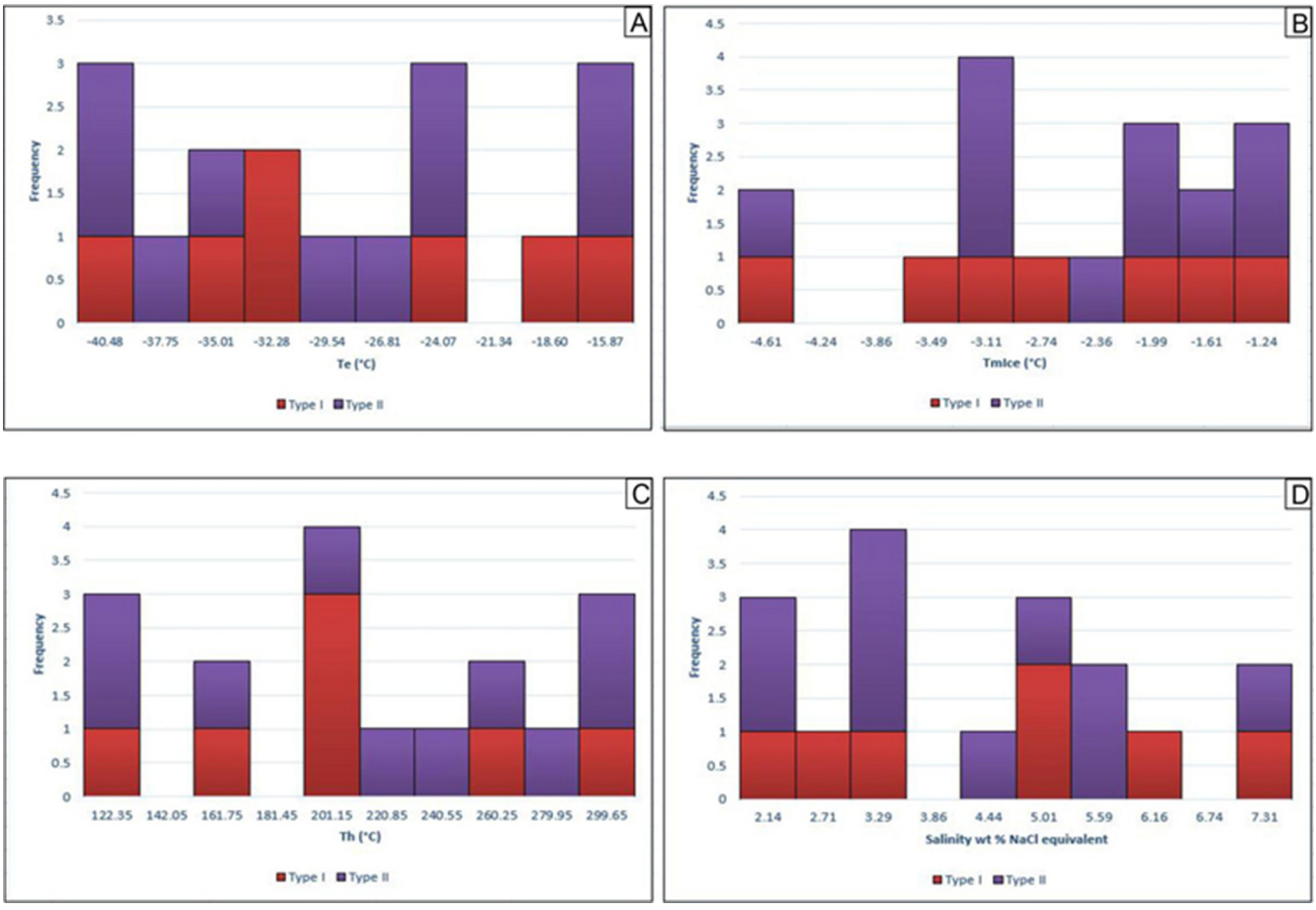

Figure 7. Type I and II fluid inclusions in the El Chucho creek. A. Eutectic temperature (Te). B. Final melt ice temperature (TmIce). C. Homogenization temperature (Th). D. Salinity (wt % NaCl equivalent).

Type II fluid inclusions: As Type I fluid inclusion, these inclusions shown the first phase change at the first melting temperature of ice from -38 to -14°C. The ice final melting temperature ranging between -5.1 to -0.9°C with an important data concentration at -3.1°C, the homogenization temperature occurs at temperature range between 100 – 139°C showing a homogenization to liquid phase too (L+V→L). The salinity calculated vary between 8.0 and 1.6 wt % NaCl (eq.) (4.8 on average) (Figure 7).

Discussion

Geologic mapping and petrographic analysis carried out on the El Chucho creek, suggest that the molybdenite and chalcopyrite mineral occurrences reported are associated with a very weak potassic hydrothermal alteration due to the presence of B-type veins and scarse shreddy secondary biotite; this high temperature alteration was overprinted mainly by propylitic and phyllic alteration. According to field relationships the mineralizing fluids analyzed seem to be related with the intrusion of minor tonalitic and quartz dioritic dykes.

The microthermal data show two different hydrothermal fluids related with the mineral occurrences.

1) The microthermometric data of Type I fluid inclusions suggest a higher temperature event that according to the diagram of Wilkinson (2001) could fit on both, an epithermal or an intrusion-related system for the study area (Figure 8), furthermore, some of the ore minerals (Py, Ccp, Mol) and hydrothermal alteration (potassic, phyllic, propylitic) found in the El Chucho creek could be related with both deposit types (Wilkinson, 2001; Camprubi *et al.*, 2003 and Hart & Goldfarb, 2005). Moreover, the interpolation of the study area over the map presented by López *et al.* (2018) shows that the study area is near (at less than ~10 km) to a prospective zone for intrusion-related deposits (Figure 9). However, some typical characteristics of intrusion-related system as the presence of fluorite, greisen alteration and the presence of CO_2 as a phase in fluid inclusions, were not observed and more importantly the presence of magnetite in the area suggest oxidized magmatism, those facts break down the hypothesis of intrusion-related but let open the possibility of an epithermal telescoped system.

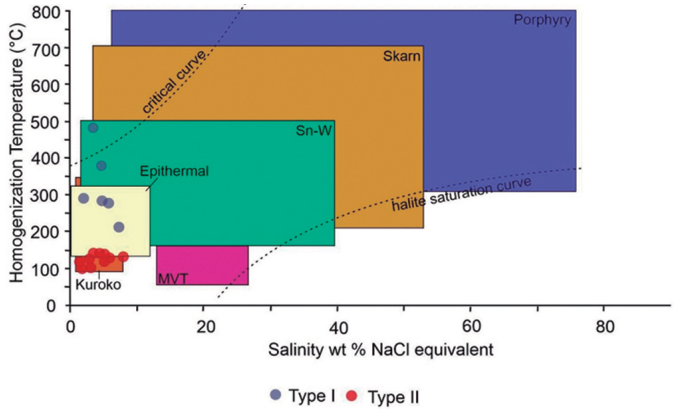

Figure 8. Diagram of typical conditions of Salinity and Homogenization Temperature for mineral deposits (Wilkinson, 2001). Note that this diagram suggests a strong relationship of the paleo-fluids analyzed (Type I and Type II) with environments of low salinity and relatively low temperature such as epithermal and kuroko deposits-types.

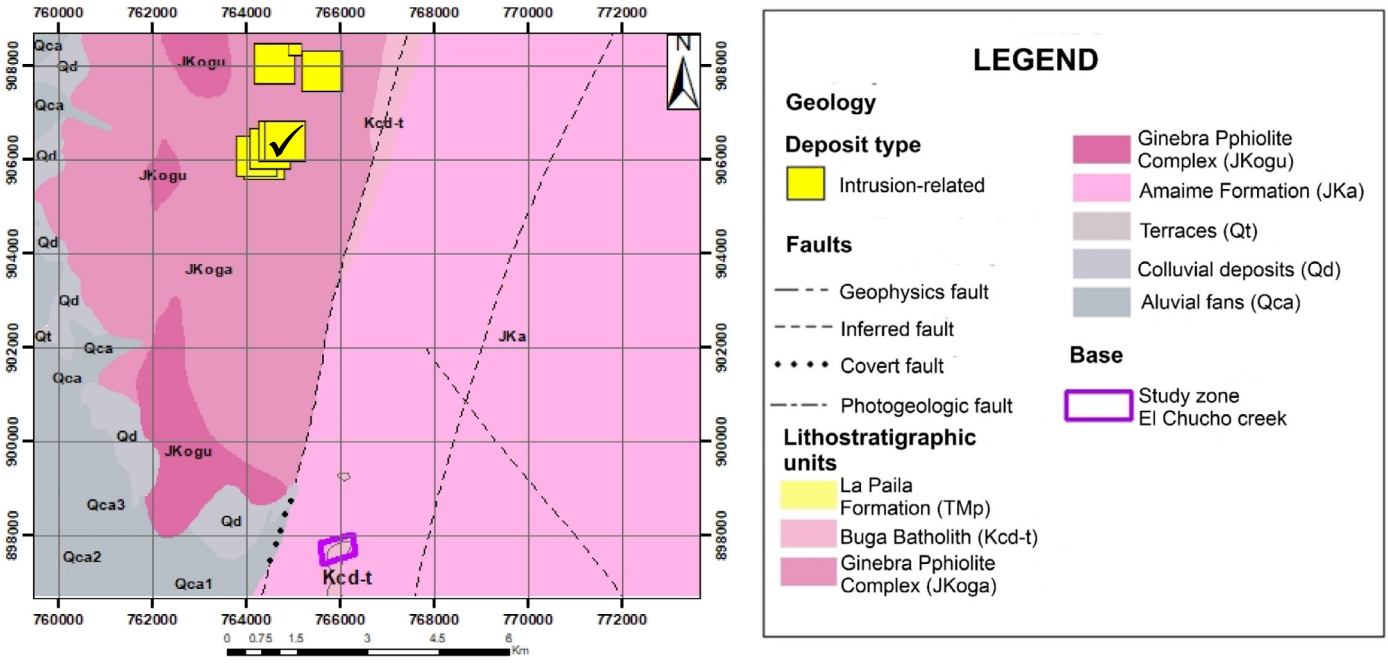

Figure 9. Intrusion-related deposits reported by López *et al.* (2018) located at the NW of the study zone. Modified from McCourt (1984) and López et.al. (2018).

2) Type II fluid inclusions show a lower temperatures that fit within the Volcanic Massive Sulphide Kuroko type deposits of Wilkinson (2001) (Figure 8) ; although the typical geometry and zonation of this deposit type as described by Ohmoto (1996) was not observed in the field, the regional geologic setting could be appropriate for this deposit type (i.e., volcanic sequences of marine origin as the Amaime Formation and Ginebra Ophiolite Complex).

Additionally, some microthermal data for Type I fluid inclusions could be interpreted as a leakage of inclusion during heating (Shepherd et.al., 1985), due to the high temperature showed without any salinity change related.

On the other hand, those different hydrothermal fluids (Type I and Type II fluid inclusions) could be related simply with a transition zone in the same hydrothermal system, this hypothesis is supported mainly by the field observations (i.e., a very weak and local presence of secondary biotite that seems related with contact zone of porphyritic dykes with the phaneritic tonalite, B-type veinlets, a frequent moderate and pervasive propylitic alteration, and a overprint of phyllic alteration structurally controlled), so according to these, the changes on fluids could obeying to the distance from the contact zone (e.g., porphyritic dykes), where the higher homogenization temperature are from those fluid inclusions related with potassic alteration on the contacts zone and lower homogenization temperature are from fluid inclusions on phyllic alteration zones.

Conclusions and recommendations

The petrography of inclusions suggest that the mineralizing fluids were trapped under low volatile content, due to the size relation of the volatile phase respect to the total size of the inclusion (L/V ratio).

According to the field observations and the differences on homogenization temperatures between the two hydrothermal fluids, we assume that mineral occurrences are related with two different hydrothermal fluids (1) of higher temperature related with the potassic alteration (secondary biotite + pyrite ± chalcopyrite ± molybdenite) close to the contact zone of porphyritic intrusions and (2) of lower temperature related with phyllic alteration (sericite + carbonate + pyrite) related with faults zones.

Due to the lack of mapping evidence on this research that support the hypothesis of any specific deposit type (intrusion-related, epithermal, VMS), is strongly suggested to carry out an extended cartography with the aim of finding any data that give support to any of those assumptions.

Acknowledgments

This research was undertaken by the project called 'Anteproyecto de investigación metalográfica, microtermométrica, geoquímica e isotópica para algunos yacimientos minerales en Colombia', that was supported by COLCIENCIAS.

The authors would like to thank the Universidad Nacional de Colombia for the technique and scientific support and for the facilities that were provided for carrying out this research. Also, we express our gratitude to Javier Gil Rodríguez and the reviewers by their invaluable contributions. In the same way, we would like to thank the people that helped during the field trip, and the laboratory technicians that supported us during sampling, preparation and analytic techniques.

References

Armas, M., (1984). Mapa geológico preliminar, Plancha 261-Tuluá, escala 1: 100.000. Ingeominas, Cali

Bakker, R. J., & Brown, P. E. (2003). *Computer modelling in fluid inclusion research.* In: I. M. Samson, A. J. Anderson, & D. D. Marshall (Eds.) Fluid Inclusions, Analysis and Interpretation Short Course (175-212). Mineralogical Association of Canada.

Bakker R. J. (2003). Package FLUIDS 1. Computer programs for analysis of fluid inclusion data and for modelling bulk fluid properties. *Chemical Geology*, 194, 3-23.

Bodnar, R. J. (1993). Revised equation and table for determining the freezing point depression of H2O-NaCl solution. *Acta Geochimica,* 57, 683-684.

Bodnar R. J. (2003a). *Introduction to fluid inclusion.* In: I. Samson, A. Anderson & D. Marshal (Eds.) Fluid inclusion analysis and interpretation. Short Course Series 32, Vancouver-British Columbia, p. 1-8.

Bodnar R. J. (2003b). *Interpretation of data aqueous-electrolyte fluid inclusions.* In: I. Samson, A. Anderson & D. Marshal (Eds.) Fluid inclusion analysis and interpretation. Short Course Series 32, Vancouver-British Columbia, p. 81-100.

Brito, R., Molano, J. C., Rodriguez, B., Dorado, C. (2010). *U-Pb LA-ICPMS dating of the Buga Batolith and associated Porphyry dykes of the*

Ginebra Ofiolite–Westernmost Central Cordillera-Colombia. VII South American Symposium on Isotope Geology, Vol. 2, Brasília, Brasil, pp. 252-256.

Camprubí, A., González, E., Levresse, G., Tritlla, J. & Carrillo, A. (2003). Depósitos epitermales de alta y baja sulfuración: una tabla comparativa. *Boletín de la Sociedad Geológica Mexicana*, Tomo LVI, No. 1, 10-18.

Cediel, F., Shaw, R. & Cáceres, C. (2003). *Tectonic assembly of the Northern Andean Block.* In: C. Bartolini, R. T. Buffler, and J. Blickwede (Eds.) The Circum-Gulf of Mexico and the Caribbean: Hydrocarbon habitats, basin formation, and plate tectonics: AAPG Memoir 79, p. 815–848.

Cediel, F. & Shaw, R. (2019). Geology and Tectonics of Northwestern South America the Pacific-Caribbean-Andean Junction. *Frontiers in Earth Sciences Springer*, 1001 pp.

Diamod, L. W. (2003). *Systematics of H2O inclusions.* In*:* I. Samson, A. Anderson & D. Marshal (Editor.) Fluid inclusion analysis and interpretation. Short Course Series 32, Vancouver-British Columbia, p. 55-78.

Einaudi, M. T. (1997). *Mapping altered and mineralized rocks. An introduction to the "Anaconda Method".* Short-course notes Stanford University, USA, 16 p.

Hart, C. J. R., & Goldfarb, R. J. (2005). Distinguishing intrusion-related from orogenic gold systems. In: Proceedings of the New Zealand Minerals Conference, Auckland, New Zealand, 125–113

Goldstein, R. H. (2003). *Petrographic analysis of fluid inclusions*. In: I. Samson, A. Anderson & D. Marshal (Eds.) Fluid inclusion analysis and interpretation. Short Course Series 32, Vancouver-British Columbia, p. 9-54.

Gustafson, L. & Hunt, J. (1975). The porphyry copper deposits at El Salvador, Chile. *Economic geology*, 70, 857–912.

Kerr, P. (1965). *Mineralogía óptica.* Ed. 3. McGraw-Hill Book Company INC, New York, 433 pp.

Leal-Mejía, H., Shaw, R. P., & Melgarejo, J. C. (2018). *Spatial-temporal migration of granitoid magmatism and the tectono-magmatic evolution of the Colombian Andes.* In: Cediel F, Shaw R. P. (Eds.) Geology and Tectonics of Northwestern South America: The Pacific-Caribbean-Andean Junction, Springer, Cham, pp 253–398.

López, J. A., Leal-Mejía, H., Luengas, C. S., Velásquez, L. E., Celada, C. M., Sepúlveda, M. J., Prieto, D. A., Gómez, M., Hart, C. J. R. (2018). Mapa Metalogénico de Colombia. Bogotá: Servicio Geológico Colombiano.

McCourt, W. (1984). Reseña explicativa del mapa geológico preliminar plancha 280 Palmira, escala 1:100.000. INGEOMINAS, Bogotá-Colombia.

Moreno-Sanchez, M., & Pardo-Trujillo, A. (2003). *Stratigraphical and sedimentological constraints on western Colombia: Implications on the evolution of the Caribbean plate*. In: C. Bartolini, R. T. Buffler, and J. Blickwede, (Eds.) The Circum-Gulf of Mexico and the Caribbean: Hydrocarbon habitats, basin formation, and plate tectonics: AAPG Memoir 79, p. 891–924.

Nivia, A. (2001). Memoria explicativa del mapa geológico del departamento del Valle del Cauca, escala: 1:250.000. INGEOMINAS. Bogotá-Colombia.

Nivia, A., Tarazona, C. & Paz, D. (2017). Geología y geocronología del Batolito de Buga y el Macizo Ofiolítico de Ginebra, Colombia. Memorias XVI Congreso Colombiano de Geología III Simposio de exploradores: Geología, sociedad y territorio. Santa Marta, Colombia.

Ohmoto, H. (1996). Formation of volcanogenic massive sulfide deposits: The Kuroko Perspective. *Ore geology reviews*, 10, 135-177.

Paz, D., Tarazona, C. & Nivia, A. (2017). *Estructuras resultantes de la evolución reológica de magmas coetáneos y de composición contrastante en el Batolito de Buga.* Memorias XVI Congreso Colombiano de Geología III Simposio de exploradores Geología, sociedad y territorio. Santa Marta, Colombia.

Raiside, R. (2003). Fluid Inclusion Analysis and Interpretation. Short Course Series 32. Vancouver. British Columbia.

Shepherd, T. J., Rankin A. H. & Alderton, D. H. M. (1985). *A practical guide to fluid inclusion studies.* Blackie, Glaslow and London. 151 p

Sillitoe, R. (1974). Tectonic segmentation of the Andes: implications for magmatism and metallogeny. *Nature,* 250, 542-545.

Streckeisen, A. L. (1976). To each plutonic rock its proper name. *Earth-Science Reviews,* 12, 1e33

Tarazona, C., Nivia, A. & Paz, D. (2017). *Evidencias de deformación sin-mágmatica en el Batolito de Buga e historia polifásica del Complejo Ofiolítico de Ginebra (Ginebra-Valle del Cauca).* Memorias XVI Congreso Colombiano de Geología III Simposio de exploradores Geología, sociedad y territorio. Santa Marta, Colombia.

Villagomez, D., Spikings, R., Magna, T., Kammer, A., Winkler, W., & Beltrán, A. (2011). Geochronoloy, Geochemistry and Tectonic Evolution of the Western and Central Cordilleras of Colombia. *Lithos,* 125, 875-896.

Wilkinson, J. J. (2001). *Fluid inclusion in hydrotermal ore deposits.* London, Journal Lithos 55, 43 p.

Whitney, D. L., & Evans, B. W. (2010). Abbreviation for names of rock-forming minerals. *American Mineralogist*, 95, 185-187.

Zhang, Y. G., & Frantz, J. D. (1987). Determination of the homogenization temperatures and densities of supercritical fluids in the system NaCl–KCl–CaCl2–H2O using synthetic fluid inclusions. *Chemical Geology,* 64, 335-350.